Early contacts between T lymphocytes and activating surfaces

2010 J. Phys.: Condens. Matter 22 194107

(http://iopscience.iop.org/0953-8984/22/19/194107)

J. Phys.: Condens. Matter **22** (2010) 194107 (12pp) doi:10.1088/0953-8984/22/19/194107

Early contacts between T lymphocytes and activating surfaces

E Cretel[1,2,3,4], **D Touchard**[1,2,3], **A M Benoliel**[1,2,3], **P Bongrand**[1,2,3,4,5] **and A Pierres**[1,2,3]

[1] INSERM UMR 600, Laboratory Adhesion and Inflammation, Parc Scientifique de Luminy, Case 937, 13288 Marseille Cedex 09, France
[2] CNRS UMR 6212, France
[3] Aix-Marseille Universités, France
[4] Assistance Publique-Hôpitaux de Marseille, France

E-mail: pierre.bongrand@inserm.fr

Received 29 October 2009, in final form 21 December 2009
Published 26 April 2010
Online at stacks.iop.org/JPhysCM/22/194107

Abstract
Cells continually probe their environment to adapt their behaviour. A current challenge is to determine how they analyse nearby surfaces and how they process information to take decisions. We addressed this problem by monitoring human T lymphocyte attachment to surfaces coated with activating anti-CD3 or control anti-HLA antibodies. Interference reflection microscopy allowed us to monitor cell-to-surface apposition with a few nanometre vertical resolution during the first minutes following contact. We found that (i) when a cell fell on a surface, contact extension was preceded by a lag of several tens of seconds. (ii) During this lag, vertical membrane undulations seemed to generate transient contacts with underlying surfaces. (iii) After the lag period, the contact area started increasing linearly with a rate of about 1.5 $\mu m^2\ s^{-1}$ on activating surfaces and about 0.2 $\mu m^2\ s^{-1}$ on control surfaces. (iv) Concomitantly with lateral surface extension, the apparent distance between cell membranes and surfaces steadily decreased. These results are consistent with the hypothesis that the cell decision to spread rapidly on activating surfaces resulted from the integration of information yielded by transient contacts with these surfaces generated by membrane undulations during a period of about 1 min.

(Some figures in this article are in colour only in the electronic version)

1. Introduction

1.1. Cell behaviour is dependent on both chemical and physical properties of their environment

Cells continually probe their environment in order to adapt immediate and long-term behaviour. Here are some examples: a macrophage may decide to phagocytize a pathogen it has just encountered, which may be completed within a few seconds (Evans 1989). A polymorphonuclear phagocyte may start migrating along a chemotactic gradient within minutes (Zigmond 1977). An anchorage-dependent cell may decide to die after being deposited on a non-adhesive surfaces, and this may occur within several hours (Chen *et al* 1997). Blood monocytes deposited on solid surfaces may begin differentiating into macrophages within a few days (Kaplan and Gaudernack 1982).

It has long been considered that cell decisions were based on the recognition of specific ligands by their membrane receptors. Thus, when melanoma cells were deposited on laminin-coated culture dishes, spreading, not attachment, was inhibited when galactosidase substrata were removed by enzymatic treatment (Runyan *et al* 1988). However, a number of recent reports demonstrated that cells are not only sensitive to biochemical signals. Indeed, their behaviour is strongly dependent on physical properties of underlying surfaces such as stiffness, micrometre- and nanometre-scale roughness, or two-dimensional topography of recognition sites (Pierres *et al* 2009). Here are some examples: (i) *substratum stiffness*. It was long ago shown

[5] Author to whom any correspondence should be addressed.

by Harris *et al* (1980) that adherent cells exerted forces on underlying substrata. More recently, it was shown that fibroblasts deposited on collagen-coated polyacrylamide gels of heterogeneous stiffness preferentially migrated toward less deformable surfaces, a property denominated as durotaxis (Lo *et al* 2000). Also, when mesenchymal stem cells were cultured on collagen-coated gels of varying cross-linking, they exhibited highly different differentiation pathways depending on the mechanical properties of the underlying surfaces (Engler *et al* 2006). (ii) *Substratum roughness*. It has long been shown that substratum roughness might influence cell adhesion. Thus, macrophages were found to accumulate on roughened areas of culture dishes (Rich and Harris 1981). More precise information could be obtained when electronic miniaturization techniques were used to deposit cells on surfaces bearing well controlled patterns. Thus, cells were found to align along grooves of micrometrical width and submicrometrical depth (Clark *et al* 1990). More recently, nanotechnologies allowed various authors such as Dalby *et al* (2002) to demonstrate that nanopillars of only 13 nm height strongly influenced protein synthesis by deposited fibroblasts. (iii) *Binding site topography*. It is now well accepted that the topography of binding sites exposed by cultured surfaces may significantly influence cell behaviour. Thus, Maheshwari *et al* (2000) showed that rat fibroblasts readily attached to substrata bearing clustered ligands of their integrin membrane receptors, but adhesion was impaired when ligand molecules were homogeneously distributed with the same surface density.

1.2. The mechanisms used by cells to analyse neighbouring structures and make behavioural choices remain poorly understood

While it is well demonstrated and accepted that cells can sense the physical and chemical properties of underlying substrata, many questions remain unanswered: (i) what kind of information is generated by the interaction between a cell and a nearby surface? (ii) How is this information translated into intracellular biochemical cascades? (iii) How are these cascades translated into a behavioural decision?

It is difficult to answer these questions because even basic terms need further analysis (Pierres *et al* 2009). Can a local change of membrane curvature, a force or a change of the 2D distribution of membrane molecules be considered as an informative event? Also, while it seems reasonable to assume that a biochemical event such as a rise of cell cytosolic calcium concentration is a significant phenomenon (Wei *et al* 2009), the link between signalling molecules and cellular outcomes was recently recognized to be poorly defined (Smith-Garvin *et al* 2009). Recording, and even defining, a cell decision is also fraught with difficulties: thus, while cell differentiation may sometimes appear as a limited sequence of fairly irreversible commitments (Gurdon and Melton 2008), much recent evidence suggests that differentiation is more flexible than was previously considered. Thus, fairly simple treatments were shown to induce a lineage switch in human neutrophils that are usually considered as terminally differentiated cells (Araki *et al* 2004). Considering short-term events, sending a filopodium along a chemoattractant gradient may be considered as an early decision, while random filopodium generation may be considered as a permanent property of some cellular states. Discriminating between both events may not be straightforward.

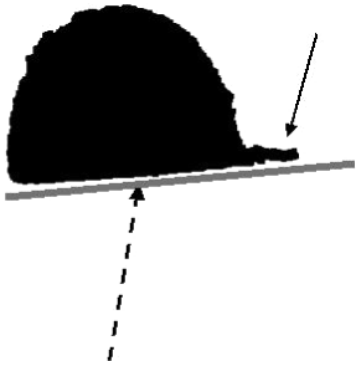

Figure 1. Cell spreading on adhesive surfaces. This figure shows the exact shape of a rat thymocyte deposited on an adherent (concanavalin A-coated) plastic surface, as shown with electron microscopy (Mége *et al* 1986). The formation of a molecular contact area involves (i) micrometre-scale flattening of a spherical cell into a truncated sphere, (ii) nanometre-scale smoothing of the rough cell surface to match the smooth plastic surface (broken arrow), (iii) active lamellipodium formation (full arrow).

In addition to the need for a careful phrasing of the addressed problem, it must be emphasized that it is very difficult to elucidate the role of a given signalling molecule due to a combination of (i) the high redundancy of intracellular phenomena, (ii) the dependence of the role of a molecule on surrounding molecules (thus, the role of a molecule is not an intrinsic property), and (iii) a multiplicity of the functions of a given molecules. See e.g. Abram and Lowell (2009) for an impressive exemplification of this situation by integrin receptors.

1.3. Cell spreading on a surface may be considered as a suitable model for studying cell decision-making

In view of the aforementioned difficulties, a suitable experimental setup to study cell decision-making should meet the following requirements: (i) the cell decision should be liable to real-time monitoring, (ii) information retrieval should be monitored sufficiently rapidly to minimize the chain of events linking cell stimulation and response, (iii) an event defined as a decision should significantly influence future cell behaviour, to ensure that it is not a random event. Arguably, cell spreading on an adhesive surface (figure 1) meets all these requirement. Indeed, while cell attachment may occur without any active cell participation (Pierres *et al* 1994), spreading does not always follow attachment and may indeed involve specific requirements (Runyan *et al* 1988, Pierres *et al* 2002). Therefore, spreading initiation requires a definite cell decision. Further, as will be shown below, spreading may be completed within a few minutes or even tens of seconds after initial contact. Finally, spreading is a highly significant event since spread and rounded cells may display quite different behaviour (Pierres *et al* 2002, Meyers *et al* 2006, Neves *et al*

2008). Interestingly, general models of spreading kinetics were recently reported (Chamaraux *et al* 2005, Cuvelier *et al* 2007).

1.4. The cell decision to spread on a surface is dependent on biochemical, chemical and physical properties of this surface

While it has long been shown that cell spreading on a surface is not a mere consequence of physical attachment and requires the presence of suitable ligands of membrane receptors (Runyan *et al* 1988), more recent results show that the physical and topographical properties of surfaces are perceived and accounted for by deposited cells. Thus, cell spreading on ligands of membrane integrins was found to require that the spacing of these ligand sites be lower than a clearcut threshold (Massia and Hubbell 1991, Calvacanti-Adam *et al* 2007). Also, a minimal substratum stiffness is required to allow spreading initiation. Fibroblast spreading on fibronectin-coated surfaces required that the substratum Young modulus be higher than 3000 kPa (Yeung *et al* 2005), and rat macrophages spread on collagen-coated glass (70 MPa Young modulus), not polyacrylamide (40 kPa, Féréol *et al* 2006). Finally, cell spreading is influenced by the roughness of the underlying surfaces (Wocjiak-Stothard *et al* 1996).

1.5. T lymphocyte spreading on activating surfaces may be considered as a workable model for visualizing cell decision

Mature T lymphocytes are known to circulate throughout living organisms and scan the surface of encountered cells to detect the presence of foreign protein fragments that are bound to major histocompatibility complex molecules of the presenting cells (see Bongrand and Malissen 1998). Even a few molecular interactions between T lymphocyte receptors (TCRs) and cognate ligands can induce a lymphocyte response, including extensive contact formation with antigen presenting cells and triggering of significant processes such as target cell destruction (Grakoui *et al* 1999). The lymphocyte decision to initiate an immune response is based on a number of parameters, including quantitative properties of TCR–ligand association (van der Merwe and Davis 2003). The mechanisms responsible for signal generation as a consequence of TCR–ligand interaction remain incompletely understood (Smith-Garvin *et al* 2009). Therefore, comparing the immediate consequences of T lymphocyte interaction with activating and non-activating surfaces might provide an useful way of analysing information-gathering and decision-making. In the present paper, we present a quantitative description of the initial interaction between T lymphocytes and activating or control surfaces. Our results provides a basis for real-time analysis of data acquisition and decision-making by individual cells.

2. Model and methods

2.1. Cells

Peripheral blood from healthy volunteers was provided by the blood bank (EFS). Peripheral blood mononuclear cells were purified by centrifugation on a density barrier following standard techniques. These cells are known to include monocytes and different lymphocyte subpopulations. In order to avoid any undesirable activation, T lymphocytes were obtained by negative selection using magnetic cell sorting (Miltenyi Biotec). It was checked with flow cytometry and CD3 labelling that more than about 85% of the remaining cells were T lymphocytes.

2.2. Surfaces

Glass coverslips were silanized and covalently coated with antibodies using glutaraldehyde chemistry, as previously described (Pierres *et al* 2008). Antibodies were either control IgG1 that were not expected to bind cells, anti-HLA (human leucocyte antigen) monoclonal antibodies (Beckman-Coulter-Immunotech, IgG1 isotype) that were expected to induce cell-substrate adhesion without activation, and anti-CD3 (UCH1, Beckman-Coulter-Immunotech, IgG1) that bound the T cell receptor/CD3 (TCR-CD3) complex on the lymphocyte membrane and were expected to trigger cell activation as well as adhesion.

Using the standard carboxyfluorescein succinimidyl ester (CFSE) labelling technique (Gett and Hodgkin 2000), it was checked that T lymphocytes deposited on anti-HLA, not anti-CD3, displayed robust proliferation after a 3-day culture (not shown).

2.3. Microscopic monitoring of early cell–surface contacts

T lymphocytes were suspended (12.5×10^6 cells ml^{-1}) in Roswell Park Memorial Institute (RPMI) 1640 culture medium supplemented with 10% foetal calf serum, 2 mM L-glutamine, 50 μM 2-mercaptoethanol, 50 U ml^{-1} penicillin and 50 U ml^{-1} streptomycin. Twenty microlitres of cell suspensions were deposited on antibody-coated coverslips on the stage of an Axiovert 135 inverted microscope (Zeiss, Germany) equipped with a heating stage set at 37 °C. Observation was performed with an antiflex™ objective and reflection interference contrast microscopy (RICM) filter block with 546 nm illumination, as previously described (Pierres *et al* 2008). Image acquisition was performed with a C4742-95-10 charged coupled device (CCD) camera (Hamamatsu, Japan). In each experiment, about 300 images were acquired with 1Hz frequency immediately after cell deposition. A single field was monitored, thus allowing us to record the immediate cell contact with the surface. A total of about 5000 images were used to record the initial contact of activating (anti-CD3-coated) surfaces with 13 individual cells and control (anti-HLA-coated) surfaces with 23 individual cells.

2.4. Image processing

The basis of our procedure was to use the zero aperture angle approximation to estimate the distance between cells and underlying surfaces (Curtis 1964, Simson *et al* 1998, Pierres *et al* 2003, 2008), yielding the following equation:

$$z = (\lambda/4\pi)\arccos[(2I - I_m - I_M)/(I_m - I_M)] \quad (1)$$

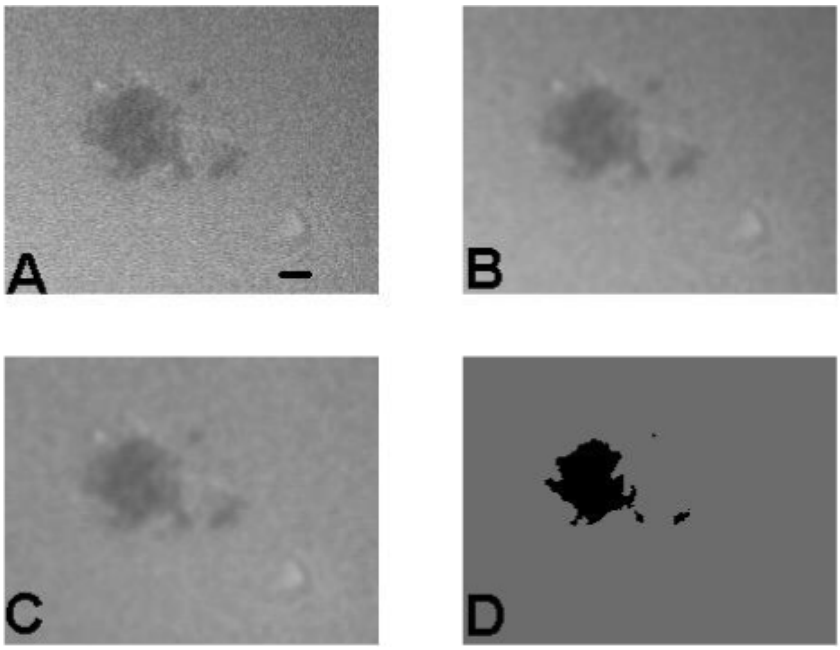

Figure 2. Image processing for contact determination. An image with a particularly high defect was selected to illustrate the requirement for basic corrections. (A) Due to the intrinsic noise of the camera, the coefficient of variation of individual pixel intensity is about 6%. In addition, illumination inhomogeneities result in a 15% coefficient of variation of average intensities between corners of the field. Performing spatial averaging (B) and linear correction for intensity variations (C) reduces the local pixel intensity variation to less than 1.5% and the overall spatial variation to less than 2%. Using equation (1) the region where the membrane-to-surface distance was estimated at less than 34 nm (Pierres *et al* 2003) was defined as the contact area and shown as a black area on (D). Bar = 2 μm.

where λ is the light wavelength in water (i.e. $546/1.33 = 410$ nm), I is the light intensity on a given pixel, and I_m and I_M are respectively the minimum and maximum intensity levels corresponding to $z = 0$ and $\lambda/4$. The interest of this formula is that it remains valid when intensities are subjected to affine transformation for contrast enhancement or when the illumination intensity fluctuates. As previously discussed (Pierres *et al* 2003, 2008), there is definite experimental support to the conclusion that this formula provides a semi-quantitative estimate of membrane-to-surface distance. In any case, it does not seem feasible to measure and even to define with nanometre accuracy the distance between a plane and a membrane studded with protrusions that may range between typically 10 and 100 nm length, which corresponds to individual molecules or membrane folds. Due to limited lateral resolution, interference microscopy is expected to yield a spatially averaged cell-to-substratum distance.

I_m and I_M were estimated by determining the ratio between the minimum or maximum and average illumination I_{av} on hundreds of images, yielding 0.77 and 1.18 for I_m/I_{av} and I_M/I_{av} respectively. A custom-made program was written to perform the following steps (figure 2).

(i) Intensity averaging was performed on 525×525 nm^2 areas to minimize camera noise.
(ii) a linear correction was performed to eliminate possible variations of illumination intensity in a box of typically 20×20 μm^2 surrounding a given cell.
(iii) The average illumination intensity was calculated in an empty area and corresponding parameters I_m and I_M were thus determined.
(iv) Equation (1) was thus used to calculate cell-to-surface separation.

Equation (1) was then used to convert microscopic images into distance maps, using coded colours to allow direct reading of cell-surface distance with nearly nanometre resolution. Sequential sequences of 8 images were then used to calculate the standard deviation of intensities at each pixel, yielding a quantitative estimate of local fluctuation amplitude. Data were used to yield fluctuation maps, as previously reported on cells (Pierres *et al* 2008) and lipid vesicles (Smith *et al* 2008).

3. Results

3.1. Quantitative analysis of contact extension

As shown on figure 3, in a typical experiment, cells were added during continuous monitoring of the microscope field and image recording with about 1 Hz frequency.

First, the evolution of the average cell–surface distance calculated on the whole cell area was studied, revealing three different kinds of behaviour as exemplified in figure 4.

- When cells were deposited on non-adhesive, IgG1-coated surfaces, they remained barely visible for minutes under the interference reflection microscopy (IRM)/RICM observation. They appeared as disks slightly brighter than empty areas. The distance calculated with equation (1) is shown in figure 4, this cannot be considered as reliable due to the ambiguity of distance calculation for values higher than about 60 nm.

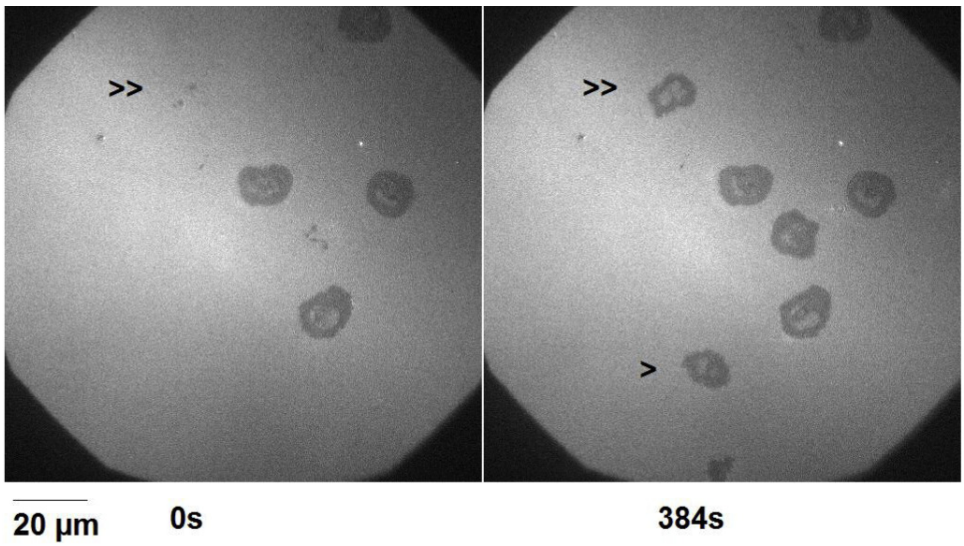

Figure 3. Real-time monitoring of contact formation between a cell and an adhesive surface. Human T lymphocytes were allowed to sediment on a surface coated with activating anti-CD3 monoclonal antibodies. During a period of 384 s, a cell was found to appear and spread on the surface (arrow). Another cell that had just sedimented at time zero (double arrow) also extensively spread during the observation period.

- When cells were deposited on adhesive non-activating surfaces (anti-HLA), contact was soon visible and the average cell–surface displayed a steady decrease after a lag on the order of 1 min.
- When cells were deposited on adhesive activating surfaces (anti-CD3), contact formation displayed a rapid increase after a lag of an order-of-magnitude duration comparable to that found on anti-HLA-coated surfaces. The lag duration displayed by individual cells varied between about 30 s and 2 min, and no significant difference could be demonstrated between the lag duration on activating and non-activating surfaces.

In order to obtain an objective definition of cell–surface contacts, the histograms of pixel brightness were determined on a series of sequential images. A typical example is shown in figure 5: during the first tens of seconds following contact, brightness histograms became bimodal, suggesting a natural intensity threshold for discrimination between free and surface-touching areas. Interestingly, the threshold of about 34 nm, that had been chosen in an earlier study made on monocyte attachment (Pierres *et al* 2003), was found to allow a fairly robust determination of contact areas, and the shape of the plots exemplified in figure 6 was only weakly dependent on the precise choice of the cutoff. Further, during the following minutes, the cell–surface distance exhibited a steady decrease, that was previously denominated as contact maturation (Pierres *et al* 2008).

Using this threshold to define contact, the kinetics of contact extension was calculated on 23 cells deposited on anti-HLA-coated surfaces and 13 cells deposited on anti-CD3-coated surfaces, yielding respectively 0.20 ± 0.04 (S.E.M.) $\mu m^2\,s^{-1}$ and 1.47 ± 0.27 (S.E.M) $\mu m^2\,s^{-1}$. Representative plots are shown in figure 6.

Thus, measuring contact extension kinetics appeared as a rapid and objective means of monitoring TCR-mediated lymphocyte activation.

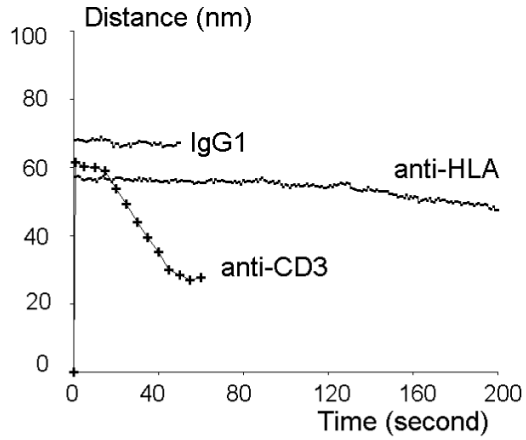

Figure 4. Kinetics of cell-to-surface interaction tightening after initial contact. The average distance between cells and surfaces was calculated with equation (1) after processing IRM/RICM images. While cell–surface distances remained higher than about 60 nm in the absence of ligand–receptor interaction (IgG1-coated surfaces), adhesive non-activating surfaces (anti-HLA) often induced a very slow decrease of distance. In contrast, anti-CD3 rapidly induced rapid contact extension. Note that time zero represents the onset of image acquisition, not cell–surface contact.

3.2. The onset of cell spreading is preceded by a formation of transient cell–surface contacts as a consequence of continual membrane undulations of nanometric amplitude

In order to obtain a better understanding of spreading initiation, a series of sequential images were processed for the determination of membrane-to-surface distance during several tens of minutes preceding and following spreading initiation. In order to convey a quantitative feeling of cell motility, the standard deviation of cell–surface distance was calculated at each pixel for a series of eight sequential values. Numerical data were displayed by building *distance maps* and *fluctuation*

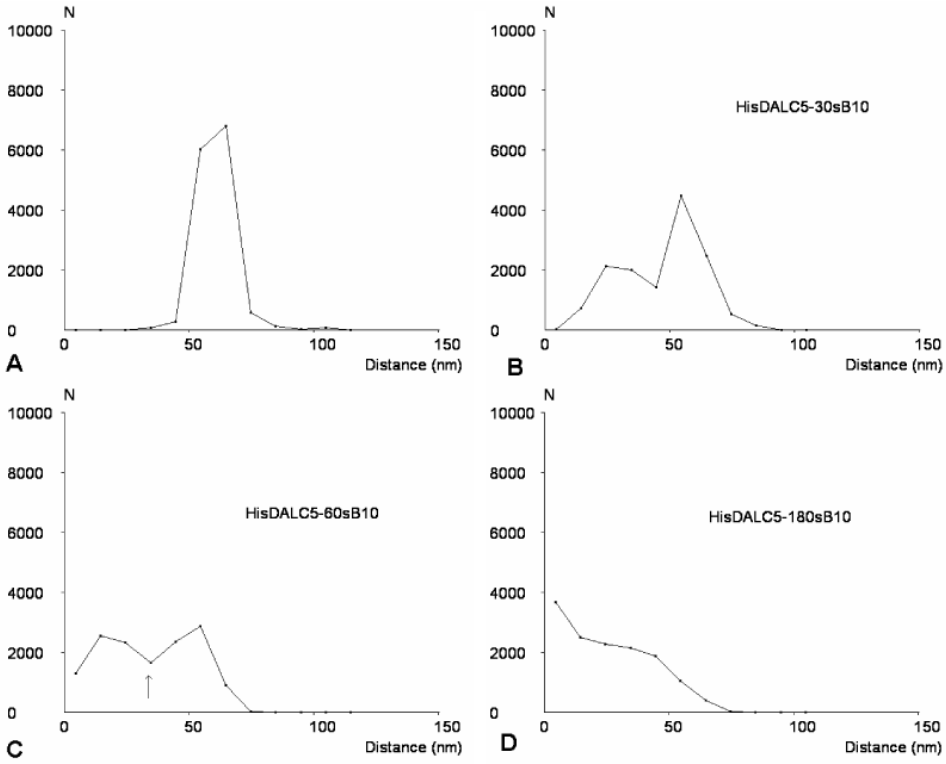

Figure 5. Contact tightening between cells and anti-CD3-coated surfaces. The histogram of average calculated distance between cells and anti-CD3-coated surfaces was calculated 30, 60 and 180 s after sedimentation. Contact first appeared as a region where the estimated cell–surface distance was lower than about 34 nm (arrow). During the following minutes, this distance displayed a steady decrease, which was defined as contact maturation.

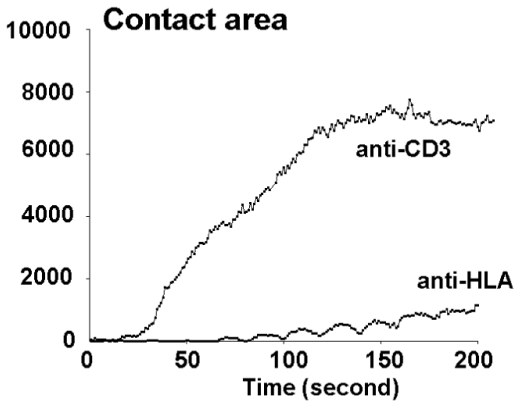

Figure 6. Spreading kinetics of T lymphocytes on activating and non-activating surfaces. Representative curves of contact extension between T lymphocytes and activating (anti-CD3) or adhesive non-activating (anti-HLA) surfaces are shown. Anti-CD3 antibodies induced rapid contact extension. Interestingly, the contact area observed between lymphocytes and anti-HLA-coated surfaces displayed slow fluctuations of about a 20 s period.

maps with coded colours. Typical images of cells falling on anti-HLA-coated (figure 7) and anti-CD3-coated (figure 8) surfaces are shown. The following conclusions were obtained:

- Cell arrival into contact with the substratum was revealed by a local increase of apparent fluctuation amplitude from about 3 nm (corresponding to background level) to 10–15 nm (figures 7(AK) and 8(AL)).
- During a lag period on the order of 1 min, cells displayed continual undulations of typically 4–6 nm amplitude with possibly transient increases to 15 nm or more (figures 7(AZ) and 8(AP)).
- These fluctuations provided a possible mechanism for the rapid formation and dissociation of transient membrane-to-surface contacts (figure 9).
- More experiments are needed to determine whether the duration of the lag period is dependent on the molecules exposed by surfaces encountered by cells.

3.3. Cell spreading involved concomitant lateral extension of contact areas and a decrease of membrane-to-surface distance

- After the lag period, the contact area started increasing quite abruptly (figures 7(BC)–(BD) and 8(AY)–(AZ)).
- While contact areas formed on anti-HLA-coated surfaces resembled fairly regular disks, contacts formed on activating anti-CD3-coated surfaces soon resembled rings with the formation of a central zone where the membrane-to-substrate distance began to increase (figures 8(BO)–(BP)).
- During the period of contact extension, vertical fluctuations of the membrane–substrate distance remained apparent. As exemplified in figure 10, a general trend was

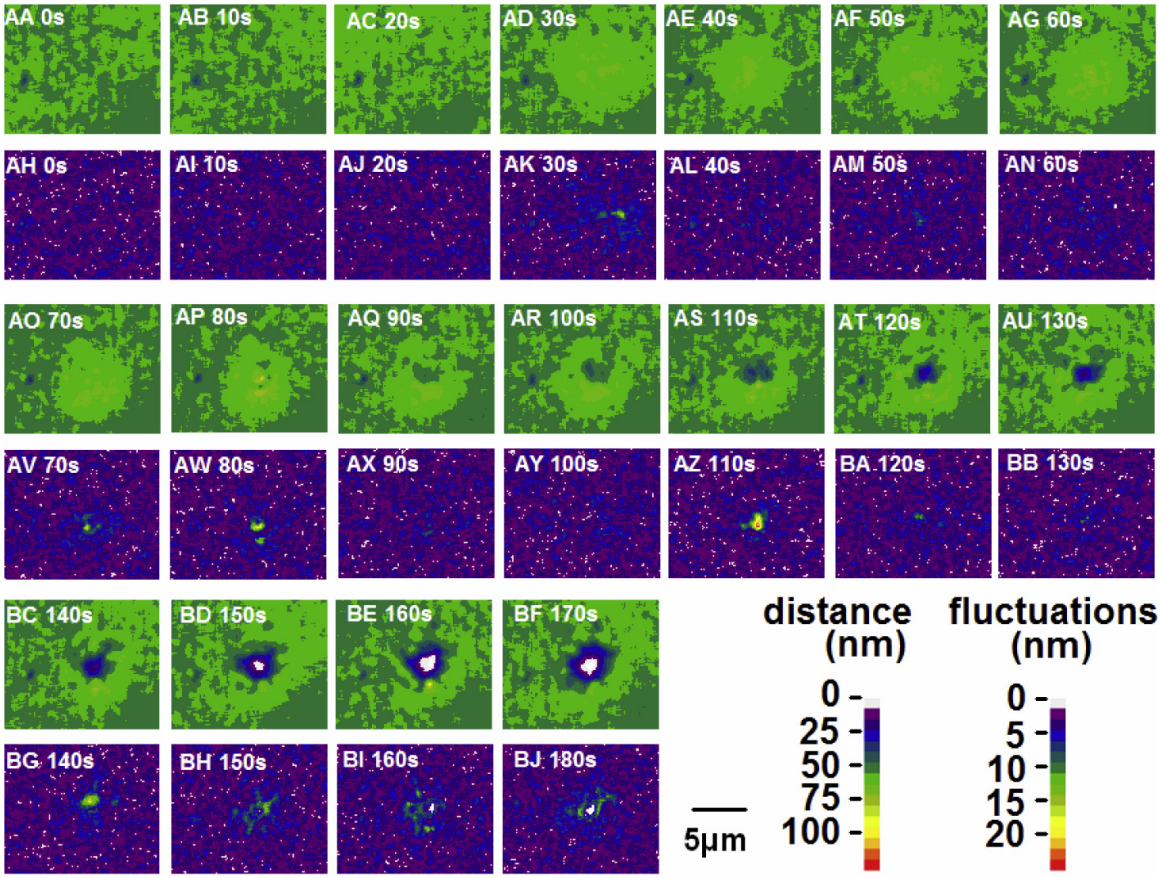

Figure 7. Spreading of a lymphocyte on a control surface. Quantification of average cell–surface distance (odd rows) and distance standard deviation (even rows) on series of sequential images reveals the cell arrival near the surface (AD/AK) and spreading initiation (AS/AZ).

that (i) the fluctuation amplitude increased when the cell–substratum distance decreased from about 50 to 10 nm and (ii) the fluctuation amplitude for membrane regions located at a given distance of the surface decreased during the first minutes following contact.

- During the first minutes following contact, the width of the gap formed between cell membranes and surface decreased by several tens of nanometres (figure 11). We compared the narrowing rate of contacts formed on control and activating surfaces by monitoring the average distance between surfaces and membrane areas that displayed 0 apparent distance at the end of each experiment. The time required for this average distance to decrease from 34 to 14 nm apparent distance was 48.2 ± 7.3 s S.E.M. ($n = 13$ cells) on activating surfaces and 75.9 ± 9.9 S.E.M ($n = 20$) on control surfaces. These results suggest that contact-narrowing was more rapid on activating surfaces.

- In order to convey an intuitive feeling for the mechanism of cell spreading, distance maps were used to build 3D drawings of the regions of the cell membrane interacting with surfaces. As shown in figure 12, results suggest that spreading involved both in-plane and perpendicular reorganization of cell membranes in contact areas.

4. Discussion

4.1. Suitability of our experimental model

The aim of our work was to describe a suitable model for understanding how a motile cell can analyse a surface it encounters and take appropriate decisions. Our strategy consisted of monitoring, as accurately as possible, the membrane deformations undergone by lymphocytes encountering control or activating surfaces. We expected to obtain two kinds of information. First, we wished to record cell–surface contacts in order to know which kind of information could be generated by the cell–surface interaction. Secondly, in view of previously reported data, the extensive membrane reorganization involved in contact extension and tightening might be considered as an early and readily detectable witness of the cell decision to undergo an activation process.

Our choice is supported by two well-accepted pieces of information. First, activating T lymphocytes with anti-CD3 antibodies is a recognized way of testing lymphocyte function in humans. Second, T lymphocytes have a need to be able to detect TCR ligands during a few minute contact with antigen presenting cells (Miller *et al* 2004), and adhesion tightening is a well known outcome of detection events, with subsequent extensive reorganization processes leading to the formation of the so-called immune synapse (Monks *et al* 1998, Grakoui *et al*

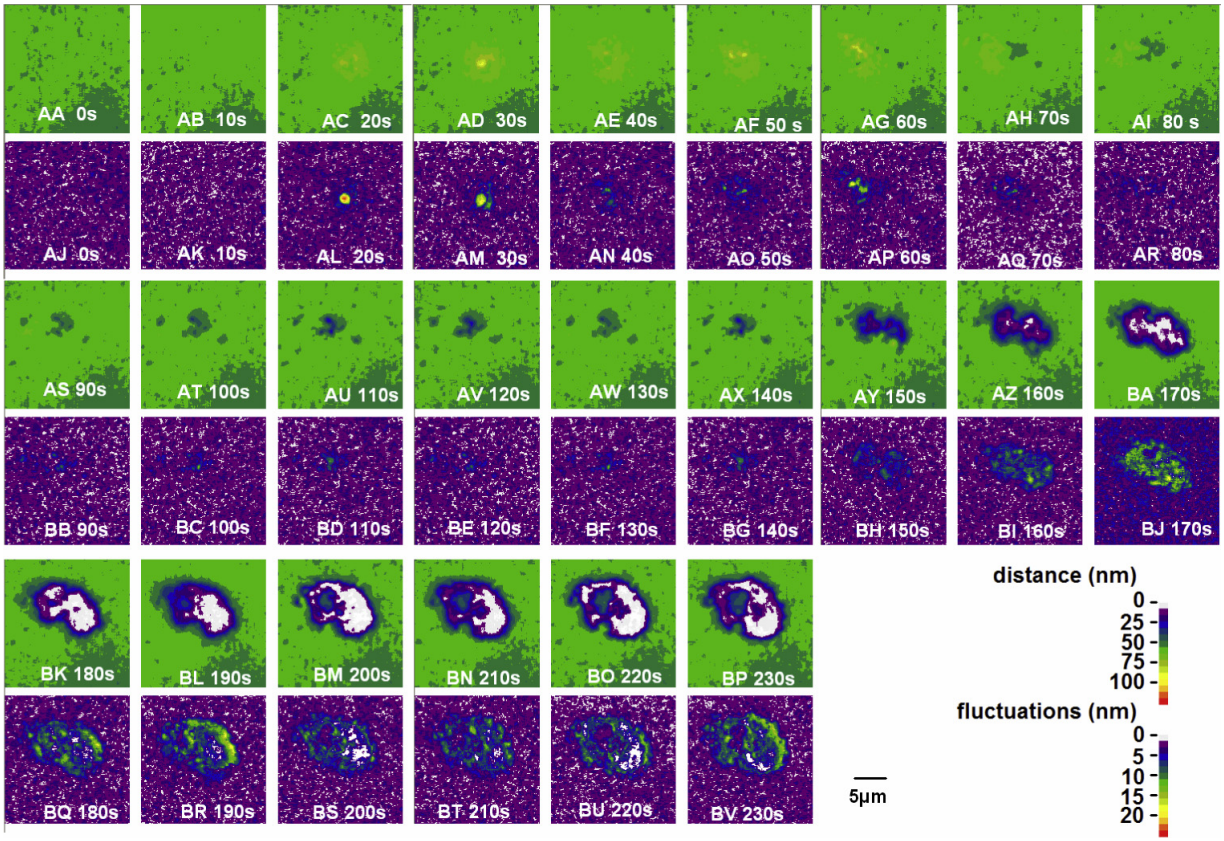

Figure 8. Lymphocyte spreading on an activating surface. The initial interaction between a lymphocyte and the anti-CD3-coated surface is shown.

1999). Therefore, both our cellular model and the measured parameters are relevant to important physiological processes.

4.2. First conclusions

The major conclusion of our study is that T lymphocytes touching an adhesive surface started spreading after a lag ranging between several tens of seconds and a few minutes. Further, the rate of lateral contact extension was between sevenfold and eightfold higher on activating (anti-CD3-coated) surfaces than on control surfaces that were not expected to trigger cell activation.

The second point is that in addition to lateral contact extension, the apparent distance between touching surfaces steadily decreased during several tens of seconds. This point may be significant in view of the reported functional significance of the width of the gap formed between immune cells and targets (McCann *et al* 2003). More work is required to confirm the finding that contact tightening was more rapid on activating than on control surfaces.

Now, it is warranted to examine some problems that will have to be considered in order to achieve a full understanding of the significance of the obtained data.

4.3. Interpretative issues

4.3.1. What is the significance of calculated cell-surface distances. While IRM/RICM has long been used to determine the distance between cell or vesicle membranes and surfaces, equation (1) cannot be expected to yield more than a semi-quantitative estimate of this distance (Pierres *et al* 2003, 2008). Indeed, while changes or absolute values of the distance between artificial bilayers and surfaces were estimated

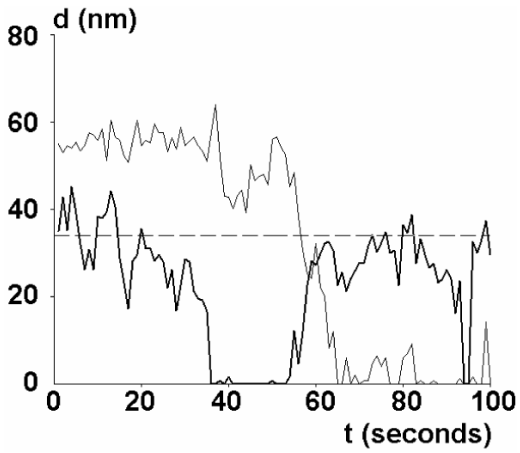

Figure 9. Membrane undulations may generate transient contacts with underlying surfaces. The thin and bold lines show the time-dependence of the distance between the (anti-CD3-coated) surface and two representative membrane areas of 0.14 μm^2. The horizontal broken line shows the threshold chosen for contact definition.

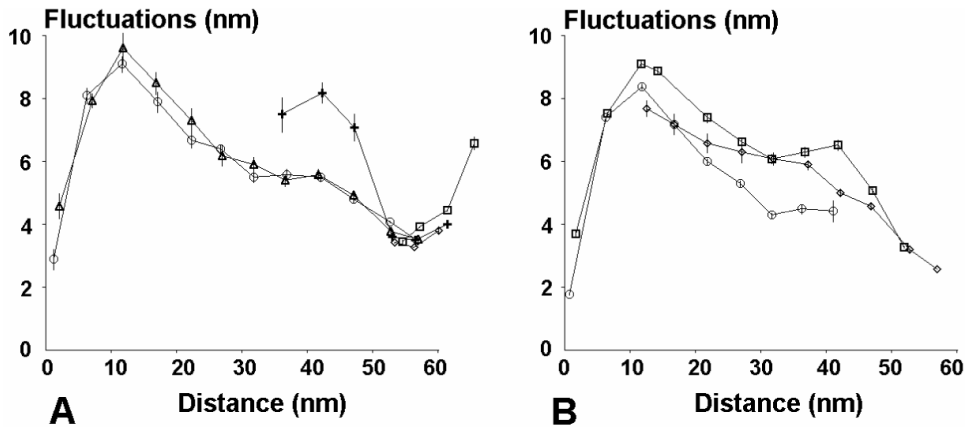

Figure 10. Variations of membrane undulations during contact formation. T lymphocytes were deposited on control anti-HLA-coated (A) or activating anti-CD3-coated (B) surfaces and the images of individual cells were monitored. During sequential periods of 7 s, the amplitude of membrane undulation was calculated and the relationship between the undulation amplitude and z coordinate was calculated. (A): time 1 s (diamonds), 30 s (squares), 110 s (crosses), 170 s (circles). (B): 1 s (diamonds), 40 s (squares), 340 s (circles). The vertical bar length is the standard error for the mean of all pixels with a comparable z coordinate.

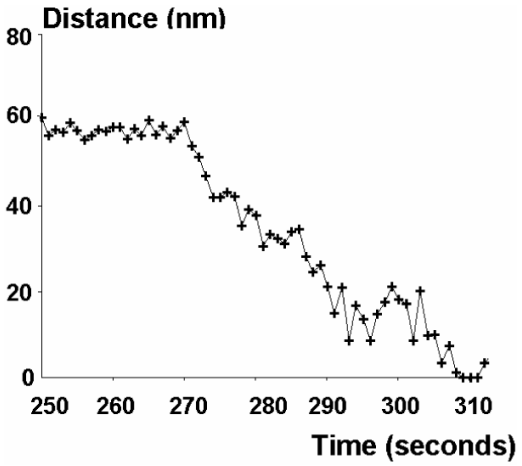

Figure 11. Decrease of membrane-to-surface distance in contact areas. A lymphocyte was deposited on an anti-CD3-coated surface and the average distance between the surface and a representative patch of 0.56 μm^2 was monitored during about 350 s. Results obtained during contact formation are shown.

to be measurable with respectively about 5 nm and 15 nm accuracy (Marx *et al* 2002), cell membranes are studded with molecules that may protrude above the bilayer by tens of nanometres: the sizes of T lymphocyte receptor, LFA-1 integrin, or the bulky CD43 molecules are about 8 nm, 20 nm and 40 nm respectively. Thus, our numerical estimates of membrane–substratum distance must be considered as relative estimates, including a notable spatial averaging. It is therefore clearly warranted to check our results with complementary methods such as total internal reflection fluorescence (TIRF; Gingell *et al* 1985), fluorescence resonance energy transfer or electron microscopy (Heath 1982). However, it must be pointed out that the conclusion that nonmuscle cells such as lymphocytes display nanometre-scale undulations is consistent with previously reported experiments made with dark field microscopy (Krol *et al* 1990) or atomic force microscopy (Pelling *et al* 2007). Therefore, while more work is required to assess the significance of our findings, it seems acceptable to conclude that lymphocyte membranes displayed nanometre-scale undulations in contact areas at the moment of initial contact and further spreading.

4.3.2. How can we detect and even define cell-surface contacts. While observations exemplified in figure 9 strongly suggest that cell membrane movements have the potential to initiate multiple contacts with neighbouring surfaces, it would be important to define these contacts and determine whether they have the capacity to generate intracellular signals. A possible means of detecting mechanical interactions between cells and surfaces would be to monitor the deformations of soft substrata underlying sedimented cells. Also, it would be attractive to monitor a number of fluorescence-based reporters of intracellular cascades (Wang *et al* 2005, Pertz *et al* 2006, Randriamampita *et al* 2008). Transient rises of intracellular calcium would be attractive candidates, since they were shown to be early markers of cell spreading (Kruskal *et al* 1986) or lymphocyte activation (Campi *et al* 2005). However, preliminary ratiometric determinations of calcium concentration with cells doubly labelled with Fluo-4 and Fura red did not reveal any conclusive correlation between calcium changes and immediate spreading initiation (not shown).

4.3.3. Are membrane undulations driven by active intercellular processes and are they influenced by ligand-coated surfaces independently of contact formation? While passive thermal processes might account for nanometre-amplitude undulations (Zidovska and Sackmann 2006), it is certainly warranted to further investigate the dependence of these movements on cell function. Indeed, in addition to the theoretical interest of this question, an attractive possibility would be that cell undulations might act as a reporter of surface detection by sedimenting cells. Thus, results displayed on figure 10 would be consistent with the hypothesis that the detection of a surface

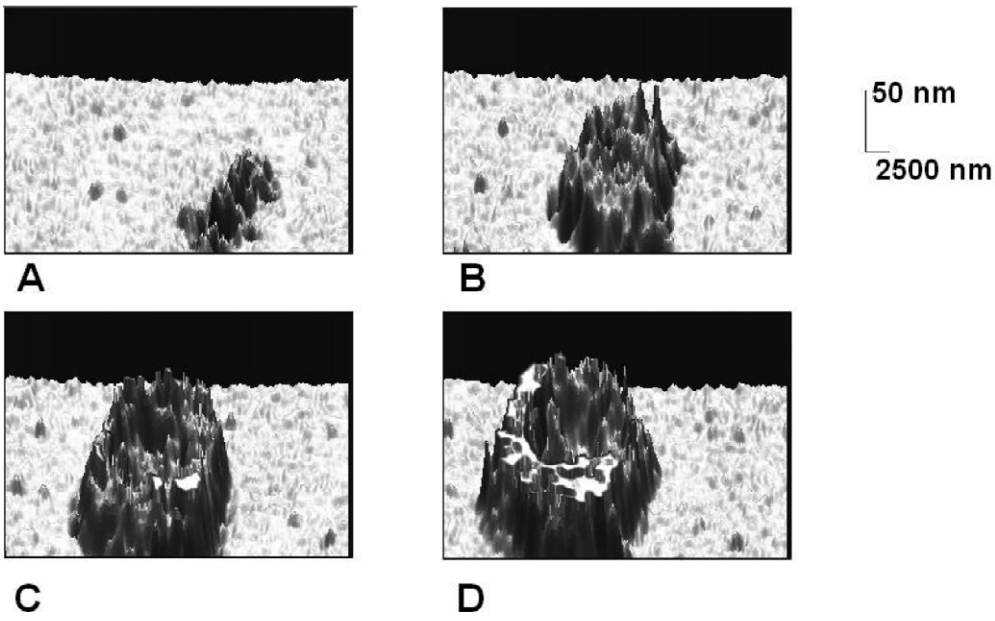

Figure 12. Membrane deformation during contact formation. Distance maps were used to build 3D images of the membrane region of a cell sedimented on an activating surface at times 1, 30, 60 and 180 s after the onset of the experiment. Different scales were used for coordinates x and y (parallel to the surface) and z (perpendicular to the surface).

at about 50 nm apparent distance by a cell might result in a change of undulation amplitude within a few tens of seconds before a tight contact occurred. A major difficulty is that it is, in principle, fairly difficult to discriminate between active and passive cell processes, since cell rheological parameters that are expected to strongly influence surface undulations are highly dependent on cell metabolism.

4.3.4. Is the spreading rate determined before the onset of spreading? An attractive interpretation of our results would be that cells might start spreading on the basis of information gathered during the nearly 1 min period of distant interaction following initial contact. This hypothesis might be tested by subjecting cells to rapid blockade or stimulation of a class of membrane receptors during the spreading phase and monitoring the effect of this treatment on the spreading rate. Indeed, it would be interesting to know the time required by cells to change their behaviour when the environment is altered. This information would be very useful to relate signalling phenomena to behavioural outcomes.

4.3.5. Is there a tight correlation between early spreading and later activation events. While experiments done at the population level clearly demonstrated that anti-CD3, not-anti-HLA, induced lymphocyte proliferation and rapid spreading, it would be informative to extend our study by monitoring, at the single cell level, the occurrence of spreading and activation markers such as CD69 or CD25 expression, interleukin 2 production and proliferation, as well as intracellular biochemical cascades when the intensity of stimulation is varied.

5. Conclusion

Here we provided a quantitative description of the shape changes displayed by T lymphocytes during the first minutes following contact formation with surfaces exposing two different ligands of their membrane molecules. We found that initial contact was followed by a lag period on the order of 1 min duration during which cell membrane undulations allowed the formation of transient molecular contacts with underlying surfaces. Then cells started extending molecular contact with a rate that was highly dependent on surface treatment. The morphology of contact areas was also markedly dependent on surface treatment. Since spreading is well recognized as a significant behavioural pattern, it is concluded that this experimental setup provides a strong basis for analysing cell information-gathering and decision-making. In addition, this might provide the basis for a rapid and innovative test of T lymphocyte function that might complement currently available ways of exploring the immune system.

Acknowledgment

This work was supported by a grant from the ARC (Association pour la Recherche sur le Cancer).

References

Abram C L and Lowell C A 2009 The ins and outs of leukocyte integrin signaling *Ann. Rev. Immunol.* **27** 339–62

Araki H, Katayama N, Yamashita Y, Mano H, Fujeda A, Usui E, Mitani H, Kohshi M, Nishii K, Masuya M, Minami N, Nobori T and Shiku H 2004 Reprogramming of human postmitotic neutrophils into macrophages by growth factors *Blood* **103** 2373–80

Bongrand P and Malissen B 1998 Quantitative aspects of T-cell recognition: from within the antigen-presenting cell to within the T cell *Bioessays* **20** 412–22
Calvacanti-Adam E A, Volberg T, Micoulet A, Kessler H, Geiger B and Spatz J P 2007 Cell spreading and focal adhesion dynamics are regulated by spacing of integrin ligands *Biophys. J.* **92** 2964–74
Campi G, Varma R and Dustin M L 2005 Actin and agonist MHC-peptide complex-dependend T cell receptor microclusters as scaffolds for signaling *J. Exp. Med.* **202** 1031–6
Chamaraux F, Fache S, Bruckert F and Fourcade B 2005 Kinetics of cell spreading *Phys. Rev. Lett.* **94** 158102
Chen S C, Mrksich M, Huang S, Whiteside G M and Ingber D E 1997 Geometric control of cell life and death *Science* **276** 1425–8
Clark P, Connolly P, Curtis A S G, Dow J A T and Wilkinson C D W 1990 Topographical control of cell behaviour: II. Multiple grooved substrata *Development* **108** 635–44
Curtis A S G 1964 The mechanism of adhesion of cells to glass *J. Cell Biol.* **20** 199–215
Cuvelier D, Théry M, Chu Y-S, Dufour S, Thiéry J P, Bornens M, Nassoy P and Mahadevan L 2007 The universal dynamics of cell spreading *Curr. Biol.* **17** 694–9
Dalby M J, Yarwood S J, Riehle M O, Johnstone H J, Affrossman S and Curtis A S 2002 Increasing fibroblast response to materials using nanotopography: morphological and genetic measurements of cell response to 13 nm-high polymer demixed islands *Exp. Cell Res.* **276** 1–9
Engler A J, Sen S, Sweeney H L and Discher D E 2006 Matrix elasticity directs stem cell lineage specification *Cell* **126** 677–89
Evans E 1989 Kinetics of granulocyte phagocytosis: rate limited by cytoplasmic viscosity and constrained by cell size *Cell Motil. Cytoskeleton* **14** 544–51
Féréol S, Fodil R, Labat B, Galiacy S, Laurent V M, Louis B, Isabey D and Planus E 2006 Sensitivity of alveolar macrophages to substrate mechanical and adhesive properties *Cell Motil. Cytoskeleton* **63** 321–40
Gett A V and Hodgkin P D 2000 A cellular calculus for signal integration by T cells *Nat. Immunol.* **1** 239–44
Gingell D, Todd I and Bailey J 1985 Topography of cell-glass apposition revealed by total internal reflection fluorescence of volume markers *J. Cell Biol.* **100** 1334–8
Grakoui A, Bromley S K, Sumen C, Davis M M, Shaw A S, Allen P M and Dustin M L 1999 The immunological synapse: a molecular machine controlling T cell activation *Science* **285** 221–7
Gurdon J B and Melton D A 2008 Nuclear reprogramming in cells *Science* **322** 1811–5
Harris A K, Wild P and Stopak D 1980 Silicone rubber substrata: a new wrinkle in the study of cell locomotion *Science* **208** 177–9
Heath J P 1982 Adhesions to substratum and locomotory behaviour of fibroblastic and epithelial cells in culture *Cell Behaviour* ed R Bellairs, A Curtis and G Dunn (Cambridge: Cambridge University Press) pp 108–77
Kaplan G and Gaudernack G 1982 *In vitro* differentiation of human monocytes. Differences in monocyte phenotypes induced by cultivation on glass or on collagen *J. Exp. Med.* **156** 1101–14
Krol A Y, Grinfeldt M G, Levin S V and Smilgavichus A D 1990 Local mechanical oscillations of the cell surface within the range 0.2–30 Hz *Eur. Biophys. J.* **19** 93–9
Kruskal B A, Shak S and Maxfield R F 1986 Spreading of human neutrophils is immediately preceded by a large increase in cytoplasmic free calcium *Proc. Natl Acad. Sci. USA* **83** 2919–23
Lo C M, Wang H B, Dembo M and Wang Y L 2000 Cell movement is guided by the rigidity of the substrate *Biophys. J.* **79** 144–52
Maheshwari G, Brown G, Lauffenburger D, Wells A and Griffith L G 2000 Cell adhesion and motility depend on nanoscale RGD clustering *J. Cell Sci.* **113** 1677–86
Marx S, Schilling J, Sackmann E and Bruinsma R 2002 Helfrich repulsion and dynamical phase separation of multicomponent bilayers *Phys. Rev. Lett.* **88** 138102
Massia S P and Hubbell J A 1991 An RGD spacing of 440 nm is sufficent for integrin alpha v beta 3-mediated fibroblast spreading and 140 nm for focal contact and stress fiber formation. *J. Cell Biol.* **114** 1089–100
McCann F E, Vanherberghen B, Eleme K, Carlin L M, Newsam R J, Goulding D and Davis D M 2003 The size of the synaptic cleft and distinct distributions of filamentous actin, ezrin, CD43, and CD45 at activating and inhibitory human NK cell immune synapses *J. Immunol.* **170** 2862–70
Mége J L, Capo C, Benoliel A M, Foa C, Galindo R and Bongrand P 1986 Quantification of cell surface roughness: a method for studying cell mechanical and adhesive properties *J. Theoretical Biol.* **119** 147–60
Meyers J, Craig J and Odde D J 2006 Potential for control of signaling pathways wia cell size and shape *Curr. Biol.* **16** 1685–93
Miller M J, Hejazi A S, Wei S H, Cahalan M D and Parker I 2004 T cell repertoire scanning is promoted by dynamic dendritic cell behavior and random T cell motility in the lymph node *Proc. Natl Acad. Sci. USA* **101** 998–1003
Monks C R F, Freiberg B A, Kupfer H, Sciaky N and Kupfer A 1998 Three-dimensional segregation of supramolecular activation clusters in T cells *Nature* **395** 82–6
Neves S R, Tsokas P, Sarkar A, Grace E A, Rangamani P, Taubenfeld S M, Alberini C M, Schaff J C, Blitzer R D, Moraru I I and Iyengar R 2008 Cell shape and negative links in regulatory motives together control spatial information flow in signaling networks *Cell* **133** 666–80
Pelling A E, Veraitch F S, Chu C P K, Nicholls B M, Hemsley A L, Mason C and Horton M A 2007 Mapping correlated membrane pulsations and fluctuations in human cells *J. Mol. Recognit.* **20** 467–75
Pertz O, Hodgson L, Klemke R L and Hahn K M 2006 Spatiotemporal dynamics of RhoA activity in migrating cells *Nature* **440** 1069–72
Pierres A, Benoliel A M and Bongrand P 2002 Cell fitting to adhesive surfaces: a prerequisite to firm attachment and subsequent events *Eur. Cell Mater.* **3** 31–45
Pierres A, Benoliel A M, Touchard D and Bongrand P 2008 How cells tiptoe on adhesive surfaces before sticking *Biophys. J.* **94** 4114–22
Pierres A, Eymeric P, Baloche E, Touchard D, Benoliel A M and Bongrand P 2003 Cell membrane alignment along adhesive surfaces: active or passive mechanism? *Biophys. J.* **84** 2058–70
Pierres A, Monnet-Corti V, Benoliel A M and Bongrand P 2009 Do membrane undulations help cells probe the world? *Trends Cell Biol.* **19** 428–32
Pierres A, Tissot O, Malissen B and Bongrand P 1994 Dynamic adhesion of CD8-positive cells to antibody-coated surfaces the initial step is independent of microfilaments and intracellular domains of cell-binding molecules *J. Cell Biol.* **125** 945–53
Randriamampita C, Mouchacca P, Malissen B, Marguet D, Trautmann A and Coffman-Lellouch A 2008 A novel ZAP-70 dependent FRET based biosensor reveals kinase activity at both the immunological synapse and the antisynapse *PLoS ONE* **3** e1521
Rich A and Harris A K 1981 Anomalous preferences of cultured macrophages for hydrophobic and roughened substrata *J. Cell Sci.* **50** 1–7
Runyan R B, Versakovic J and Shur B D 1988 Functionally distinct laminin receptors mediate cell adhesion and spreading: the requirement for surface galactosyltransferase in cell spreading *J. Cell Biol.* **107** 1863–71

Simson R, Wallraff E, Faix J, Niewöhner J, Gerish G and Sackmann E 1998 Membrane bending modulus and adhesion energy of wild-type and mutant cells of dictyostelium lacking talin or cortexillins *Biophys. J.* **74** 514–22

Smith A-N, Sengupta K, Goennenwein S, Seifert U and Sackmann E 2008 Force-induced growth of adhesion domains is controlled by receptor mobility *Proc. Natl Acad. Sci. USA* **105** 6906–11

Smith-Garvin J E, Koretzky G A and Jordan M S 2009 T cell activation *Ann. Rev. Immunol.* **27** 591–619

van der Merwe P A and Davis S J 2003 Molecular interactions mediating T cell antigen recognition *Annu. Rev. Immunol.* **21** 659–84

Wang Y, Botvinick E L, Zhao Y, Berns M W, Usami S, Tsien R Y and Chien S 2005 Visualizing the mechanical activation of Src *Nature* **434** 1040–5

Wei C, Wang X, Chen M, Ouyang K, Song L-S and Cheng H 2009 Calcium flickers steer cell migration *Nature* **457** 901–4

Wocjiak-Stothard B, Curtis A, Monaghan W, MacDonald K and Wilkinson C 1996 Guidance and activation of murine macrophages by nanometric scale topography *Exp. Cell Res.* **223** 426–35

Yeung T, Georges P C, Flanagan L A, Marg B, Ortiz M, Funaki M, Zahir N, Ming W, Weaver V and Janmey P A 2005 Effects of substrate stiffness on cell morphology, cytoskeletal structure and adhesion *Cell Motil. Cytoskeleton* **60** 24–34

Zidovska A and Sackmann E 2006 Brownian motion of nucleated cell envelopes impedes adhesion *Phys. Rev. Lett.* **96** 048103

Zigmond S H 1977 Ability of polymorphonuclear leukocytes to orient in gradients of chemotactic factors *J. Cell Biol.* **75** 606–16